Published in final edited form as:
Acad Radiol. 2011 November ; 18(11): 1341–1348. doi:10.1016/j.acra.2011.06.013.

Disposition of ultrasound sensitive polymeric drug carrier in a rat hepatocellular carcinoma model

Michael C. Cochran, BS, **John R. Eisenbrey, PhD**, **Michael C. Soulen, MD**, **Susan M. Schultz, RDMS**, **Richard O. Ouma**, **Sarah B. White, MD**, **Emma E. Furth, MD**, and **Margaret A. Wheatley, PhD**
School of Biomedical Engineering Science and Health Systems, Drexel University, Philadelphia, PA (MCC, JRE, ROO, MAW); Division of Interventional Radiology, University of Pennsylvania, PA, (MCS, SBW); Department of Radiology, University of Pennsylvania (SMS); Division of Hepatopathology, University of Pennsylvania PA, (EEF)

Abstract

Rational and Objectives—A doxorubicin-loaded microbubble has been developed that can be destroyed with focused ultrasound resulting in fragments, or “nanoshards” capable of escaping through the leaky tumor vasculature, promoting accumulation within the interstitium. This study utilizes a rat liver cancer model to examine the biodistribution and tumoral delivery of this microbubble platform compared with de novo drug-loaded polymer nanoparticles and free doxorubicin.

Methods—Microbubbles (1.8μm) and 217nm nanoparticles were prepared containing 14-C labeled doxorubicin. Microbubbles, nanoparticles, a combination of the two, or free doxorubicin were administered intravenously in rats bearing hepatomas, concomitant with tumor insonation. Doxorubicin levels in plasma, organs and tumors were quantified after 4hours, 7 and 14days. Tumors were measured upon sacrifice and evaluated with autoradiography and histology.

Results—Animals treated with microbubbles had significantly lower plasma doxorubicin concentrations (0.466±0.068%/ml) compared with free doxorubicin (3.033±0.612%/ml, p=0.0019). Drug levels in the myocardium were significantly lower in animals treated with microbubbles compared to free doxorubicin (0.168%/g tissue vs. 0.320%/g, p=0.0088). Tumors treated with microbubbles showed significantly higher drug levels than tumors treated with free doxorubicin (2.491±0.501 %/g vs. 0.373±0.087 %/g, p=0.0472). These tumors showed significantly less growth than tumors treated with free doxorubicin (p=0.0390).

Conclusions—Doxorubicin loaded microbubbles triggered with ultrasound provided enhanced, sustained drug delivery to tumors, reduced plasma and myocardium doxorubicin levels and arresting tumor growth. The results offer superior treatment than injection of de novo synthesized nanoparticles.

Keywords

Ultrasound contrast agent; targeted drug delivery; hepatocellular carcinoma; nanoparticles

Correspondence to: M.A. Wheatley PhD, School of Biomedical Engineering Science and Health Systems, Drexel University, Philadelphia, PA 19104 (fax: 215.895.5837, phone: 215.895.2232, wheatley@coe.drexel.edu).

INTRODUCTION

The hyperpermeable vasculature of a tumor created during angiogenesis is characterized by pore sizes ranging from 380–780 nm, allowing nanoparticles (NP) to extravasate into the interstitium (1–2). Additionally, the tumor architecture generally lacks adequate lymphatic drainage, allowing these particles to accumulate over time (3).

Ultrasound contrast agents (UCA) are small (generally 1–6 μm) gas bubbles encapsulated within a stabilizing shell. When the agent is exposed to ultrasound, the gas core of the agent will expand and contract with a wall velocity on the order of hundreds of meters per second (4). These agents are generally restricted to circulation within the vascular system due to their size, but are small enough to penetrate into angiogenic vessels (5). When an UCA is exposed to sufficient ultrasound intensity the agent can cavitate and create enough shear force to rupture cell membranes and increase the permeability of the capillary wall, allowing particles to escape the vessel and penetrate tens of microns into the tumor interstitium (6–7). Vascular permeability can be enhanced through the use of an UCA combined with targeted ultrasound (8).

Several groups have been developing drug loaded UCAs that can release drug when triggered by ultrasound at the desired target. Doxorubicin (Dox) has been loaded onto the surface of phospholipid microbubbles through electrostatic interactions (9) and into stabilized micelles (10). Insonated polymeric micelles were able to substantially increase drug accumulation within tumor cells in an *in vivo* ovarian cancer tumor model (11). Ferrara's group suggests that micelles and phospholipid microbubbles have limited drug payloads due to their thin shells, making them an inefficient delivery vehicle and proposed the use of drug-loaded liposomes conjugated to microbubbles to increase payload (12). Micelles are unstable below their critical micelle concentration which can result in a premature release of drug (13). Additionally, Dox loaded liposomes have been associated with dose limiting systemic side effects (14).

Polymer shelled UCAs with thicker (100–400 nm) walls may be a useful alternative for targeted drug delivery (15–16). Dox-loaded UCAs with a poly(lactic acid) (PLA) shell and an air core have been developed (16–17). *In vitro*, these agents have shown significantly greater antitumor activity when triggered with ultrasound (18). Exposure to ultrasound significantly reduces the size to below 400 nm (19) due to fragmentation of the shell. We propose that the resulting nanoshards are capable of escaping leaky tumor vasculature and accumulating within the interstitium where the polymer fragments can degrade and provide a sustained, localized release of Dox (figure 1). We also proposed that ultrasound will facilitate the deposition of the fragments in the tumor, resulting in a more rapid accumulation compared to that of conventional NP, which have minimal response to ultrasound. Similar proof of concept studies in VX2 implanted rabbits have shown a 110% increase in Dox delivered to the tumor when insonated, relative to a non-insonated control (19).

Dox has successfully been used to treat various types of solid tumors including those arising in the breast, bile ducts, endometrial tissue and liver (20). However, the systemic delivery of Dox has been associated with cardiotoxic effects including cardiac arrhythmias and congestive heart failure which have limited its use and created a need for targeted delivery systems (21). A variety of alternative strategies for delivering Dox and reducing cardiotoxic effects are being investigated. Dox has been encapsulated within liposomes (22) resulting in the FDA approved formulation Doxil® (14) polymeric micelles (23) and other formulations of NP (24) that can accumulate within tumors via the enhanced permeability and retention (EPR) effect (1).

This paper compares biodistribution, Dox delivery and short term tumor response of three drug delivery platforms in a rat liver cancer model. Dox-loaded PLA UCAs are compared with free Dox, Dox-loaded NP, and a combination of NP and UCAs. The combination was used to investigate if there are any effects on NP delivery enhanced by co administered UCA capable of cavitating in the ultrasound beam and enhancing vascular permeability as mentioned above.

Materials and Methods

Materials

The following suppliers were used: PLA (100 DL MW = 83 KDa), Lakeshore Biomaterials (Birmingham, AL), camphor, Sigma-Aldrich (St. Louis, MO), ammonium carbonate, J.T. Baker (Phillipsburg, NJ), Poly(vinyl alcohol) (88% mole hydrolyzed, MW = 25 KDa), Polysciences (Warrington, PA), radiolabeled (14C) Dox, GE Healthcare (Piscataway, NJ), tissue solvent (Soluene-350), Perkin Elmer (Waltham, MA), RPMI 1640 and Trypsin (0.25% Trypsin/2.21mM EDTA), Mediatech Inc. (Manassas, VA), hematoxylin and eosin, VWR (Bridgeport, NJ), methylene chloride, isopropyl alcohol, hexane, fetal bovine serum, hydrogen peroxide, liquid scintillation counting (LSC) cocktail and optimal cutting temperature (OCT) compound, Fisher Scientific (Waltham, MA).

Microbubble Fabrication

Dox loaded UCA were prepared by a double emulsion technique described in the literature (16). Five hundred milligrams of poly(lactic acid) and 50 mg of camphor were dissolved in 10 ml of methylene chloride. Fifteen milligrams of 14C-labeled Dox and 1 ml of 4% w/v ammonium carbonate were added and sonicated at 20 kHz for 30 seconds in an ice water bath with 3 seconds on and 1 second off at 110 W (Misonix Inc. CL4 probe, Farmingdale, NY). The resulting emulsion was added to 50 ml of 5 % w/v poly(vinyl alcohol) at 4 °C then homogenized at 9500 rpm for 5 min with a saw tooth homogenizer (Brinkmann Instruments, Westbury, NY). Afterwards, 100 ml of 2% isopropyl alcohol was added and stirred for 1 h to allow the solvent to evaporate. The agent was then collected by centrifugation at 2500g for 5 min and washed three times with hexane to remove any residual solvent. After allowing any remaining hexane to evaporate, the agent was flash frozen and lyophilized for 48 hours with a Virtis Benchtop freeze dryer (Gardiner, NY). When exposed to atmospheric pressure, voids created by lyophilization filled with air, yielding the UCA containing Dox. These agents have previously been characterized with dynamic light scattering and scanning electron microscopy and shown to have a mean particle size of 1.865 ± 1.074 μm, a polydispersity index of 0.308 ± 0.102 and a resonance frequency near 5 MHz (12).

Nanoparticle Fabrication

Dox loading in solid polymer NP generated by a single emulsion is limited due to the low lipophilicty of Dox (25) making it necessary to load the NP used in this study by a wet absorption method. Dox-loaded NP were fabricated by first producing PLA NP by a single emulsion method followed by surface adsorption of Dox. Two hundred milligrams of PLA dissolved in 5 ml of methylene chloride were sonicated similar to the UCAs at 75 W of applied power. After sonication, the emulsion was formed by adding the polymer solution to 100 ml of 1% w/v poly(vinyl alcohol) and homogenizing at 12,500 rpm for 7.5 min. The emulsion was stirred for 12 h to allow methylene chloride evaporation. NP were then collected by centrifugation at 12,500g for 1 hour (Sorvall WX ultracentrifuge, AH-629 rotor, Thermo Electron Corp, Waltham, MA). The supernatant was discarded and the pellet flash frozen and lyophilized. NP were suspended in a 3% w/v 14C labeled Dox/phosphate buffered saline solution and stirred end over end at 4 °C for 24 hours. NP were then washed 3 times with deionized water, collected by centrifugation and lyophilized. The NP were

characterized with dynamic light scattering and shown to have a mean particle size of 217 ± 88 nm.

Cell Culture

The Morris hematoma 3924a cell line was a generous gift from Dr. Uwe Haberkorn at the German Cancer Research Center in Heidelberg, Germany. Cells were grown in RPMI 1640 medium, supplemented with 20% (v/v) fetal bovine serum. Cells were maintained in a humidified incubator at 37 ° C in a 5% CO_2 atmosphere. Testing for pathogens was performed by Research Animal Diagnostic Laboratory (Columbia, MO) to show the cell line was pathogen free before used in animals.

Animals

Sixty three 200–300 g ACI rats were purchased from Harlan Laboratories (Somerville, NJ). Animals were housed in accordance with the Guide for the Care and Use of Laboratory Animals. All animal studies described here were performed in accordance with the guidelines of the author's institution's Institutional Animal Care and Use Committee.

Tumor Implantation

A subcutaneous tumor was induced by suspending 5×10^6 cultured Morris 3924a hepatoma cells in 100 µl of serum free RPMI 1640 medium followed by a subcutaneous injection into both flanks of 4 carrier rats as described by Maataoui et al. (26). The subcutaneous tumors were harvested after 3 weeks and minced into cubes approximately 1–2 mm^3. Tumor implantation was performed as described by Yang et al. (27). Under isoflurane anesthesia, rats underwent a 15 mm subxiphoid midline abdominal incision. The left lateral lobe of the liver was retracted out of the abdominal and a small stab wound was made with a scalpel. Gelatin sponge (Pfizer Inc, NY, NY) was inserted into the cavity for 1–2 min while manual compression was held to attain hemostasis. The sponge was replaced by a 1–2 mm^3 piece of tumor inserted into the cavity. The left lobe was returned to the peritoneal cavity and the abdominal wall and skin closed with sutures. Tumors were then grown for 2–3 weeks prior to treatment

Treatments

Anesthetized rats were scanned with an ATL/Philips HDI-5000 scanner (Bothel, WA) using a linear 12-5 MHz transducer. Initial tumor measurements were obtained in the transverse and sagittal planes. With the transducer focused on the tumor, a 1 ml aliquot of saline containing a suspension of one of the four treatments was injected through an intravenous catheter placed in the tail vein, followed by 1 ml of a saline flush. The tumor was continuously insonated following the injection for 20 min with Doppler ultrasound at a mechanical index of 0.40–0.45 and a pulse repetition frequency of 1000 Hz. Each particle treatment consisted of injection of 12 mg of total polymer, a quantity that we have found to have minimal adverse effects. This resulted in Dox levels of 167 µg, 34µg (maximum achievable loading for NP), 100 µg and 112 µg for UCA, NP, combinations and free drug respectively. Quantities were chosen to ensure equal weights of polymer injected. Biodistributions are quoted as % initial dose to allow for comparison between platforms.

Plasma Doxorubicin Quantification

Plasma Dox levels were measured over 30 minutes after injection. Blood samples of approximately 0.5 ml were collected through the tail vein catheter at 0, 5 15 and 30 minutes and centrifuged for 3 min at 2000 g in BD Microtainer® tubes (Franklin Lakes, NJ) to isolate plasma. Two hundred microliters of plasma were added to 1 ml of a 1:1 mixture of Soluene-350 tissue solvent and isopropyl alcohol and incubated at 60 °C for 2 hours. Two

hundred microliters of 30% v/v hydrogen peroxide was added to the cooled samples and shaken for 30 min followed by incubation at 60 °C for an additional 30 min. Liquid scintillation counting cocktail (15 ml) was added to the cooled mixture. After 1 hour, samples were read in a 1500 TRI-CARB liquid scintillation analyzer (Packard Instruments, Downers Grove, IL). For each point n = 5 from each of the four experimental groups.

Organ Doxorubicin Quantification

Dox levels in the organs and tumor were measured at 4 hours, 7 days or 14 days after treatment. After sacrifice the spleen, myocardium, lungs, right and left lobes of the liver and the tumor were removed and three 50–100 mg sections were collected from each. Samples were weighed, added to 2 ml of Soluene-350 tissue solvent and incubated for 3.5 hours at 60 °C to dissolve the tissue. The solutions were then processed identically to plasma samples. For all treatments n = 3 at each time point except for free

Dox and for UCA at 7 days which had n=2 due to lack of tumor development in some animals.

Tumor Growth Measurements

Tumor size at the time of treatment was measured by ultrasound from transverse and sagittal planes, and at harvest by caliper. The largest diameter measured at the time of sacrifice was normalized to the largest diameter measured by ultrasound at the time of treatment.

Histology and Autoradiography

Sections of tumors were embedded in optimal cutting temperature media and frozen on dry ice then stored at −80 °C. Sections (10 μm) from tumors were used for autoradiography and stained with hematoxylin and eosin. Autoradiography was performed to determine the drug distribution within the sections. A phosphor plate (Fujifilm, Valhalla, NY) was exposed to tumor sections for 3 weeks. Plates were read with a Fujifilm FLA-7000 digital imager (Valhalla, NY). Liver and tumor histology was reviewed by an experienced hepatopathologist.

Statistical Analysis

Statistical significance for multiple groups was assessed using a one way ANOVA and individual groups were compared using a Student's t-test ($\alpha = 0.05$) using Prism 5 (GraphPad, San Diego, CA). Values are reported as the mean ± standard error about the mean. Error bars were displayed as standard error about the mean.

Results

Plasma Doxorubicin Levels

Dox plasma levels are shown in figure 2 for each of the four treatments. Values are plotted as % of injected dose (%ID) to account for the fact that NP loaded to the maximum possible were carrying a lower drug load. Plasma drug levels were highest, as measured at the 5 minute sample for all four treatments with significantly higher % of total dose for unencapsulated free Dox (3.033 ± 0.612 %ID/ml plasma, compared to all other groups: UCA (0.466 ± 0.068 %ID/ml plasma), NP (1.650 ± 0.294 %ID/ml plasma) and the combination of UCA and NP (0.632 ± 0.046 %ID/ml plasma, $p<0.0470$). Dox loaded NP also lead to a significantly greater percentage of injected drug in the plasma after 5 minutes compared to drug encapsulated within UCA (1.650 ± 0.294 %ID/ml plasma vs. 0.466 ± 0.068 %ID/ml plasma, $p=0.0052$). After 15 minutes plasma drug levels remained

significantly greater for free Dox compared to drug encapsulated within UCA 1.151 ± 0.422 %ID/ml plasma, vs. 0.242 ± 0.030 %ID/ml plasma, p= 0.0395).

Organ and Tumor Doxorubicin Levels

Organs and tumors harvested from rats sacrificed 4 hours, 7 days and 14 days after treatment were processed and used to determine the Dox biodistribution and persistence for each of the four treatments (Figure 3). After 14 days, drug levels in the spleen remained significantly greater for rats treated with UCAs 4.833 ± 1.00 %ID/g tissue and for the combination of NP and UCAs 6.842 ± 1.280 %ID/g compared to rats treated with free Dox 0.283 ± 0.006 %ID/g ($p<0.0210$) as shown in figure 3A. Drug levels in the right and left lobes of the liver are shown in figures 3B and 3C respectively. After14 days, drug levels in the left lobe of the liver were greater for rats treated with UCAs 2.381 ± 0.458 %ID/g and the combination of NP and UCAs 2.945 ± 0.465 %ID/g (compared to rats treated with free Dox 0.177 ± 0.006 %ID/g ($p<0.0159$). After 14 days there were no significant differences in Dox levels in the lungs for any of the treatments compared to free Dox (Figure 3D). After 14 days, the percentage of injected Dox in the myocardium of rats treated with NP remained significantly higher than those treated with free Dox (0.736 ± 0.097 %ID/g tissue, vs. 0.320 ± 0.054 %ID/g tissue, p=0.0292) while those treated with UCA were significantly lower compared to free Dox (0.168 ± 0.017 %ID/g tissue, vs. 0.320 ± 0.054 %ID/g tissue, p=0.0088) as shown in figure 3E. Dox loaded UCAs resulted in the most efficient delivery of drug into the tumor, with significantly greater levels of Dox in tumors treated with UCA compared to tumors treated with free Dox as shown in figure 3F (2.491 ± 0.501 %ID/g tissue, vs. 0.373 ± 0.087 %ID/g tissue, p= 0.0472).

In rats treated with UCAs the drug levels were highest for all organs in the 4 hour samples with 13.291 ± 0.884 %ID/g in the spleen, 5.118 ± 0.704 %ID/g in the right lobe of the liver, 5.751 ± 0.774 %ID/g in the left lobe of the liver, 1.507 ± 0.496 %ID/g in the lungs, 0.330 ± 0.021 %ID/g in the myocardium and 2.491 ± 0.501 %ID/g in the tumor as shown in figure 4. After 14 days, drug levels in the spleen, liver, lungs and myocardium were all significantly lower compared to samples taken at 4 hours ($p<0.0212$) while drug levels in the tumor showed no significant drop from day 0 to day 14 (2.491 ± 0.501 %ID/g vs 2.076 ± 1.079%ID/g, p=0.7).

Tumor Growth

Normalized tumor growth is shown in figure 5. There were no significant changes in tumor size from the time of treatment to 7 days post treatment for any of the four treatment groups. Tumors treated with UCAs showed no significant change in size from day 0 to day 14 (p=0.3) while tumors treated with free Dox showed a significant increase in size (p=0.0437). After 14 days, tumors treated with UCAs were significantly smaller than tumors treated with free Dox (p=0.0390). This was primarily a short term, biodistribution study and hence no untreated groups were in the incorporated. However it was noted that tumors treated with NP or the combination of UCAs and NP showed no significant difference compared to tumors treated with free Dox (p=0.1 and p=0.3), although UCAs had a greater drug carrying capacity compared to equal polymer weights of NP (167, 34, and 100 μg total Dox for contrast agent, NP and combination platforms respectively).

Autoradiography and Histology

Liver histology was normal in all groups at all time points. Tumors had patchy areas of necrosis involving 25% –50% of the slide area at all time points, without clear cut differences among the groups.

Autoradiography images of frozen tissue sections from each treatment and time point are shown in figure 6. Tumors treated with UCAs showed the greatest accumulation of drug at 4 hours, predominantly around the periphery, while tumors treated with NP or free Dox showed no detectable drug at any time point. Tumors treated with UCA and the combination of NP and contrast agent maintained detectable drug levels after 14 days.

Discussion

UCAs have attracted interest for site specific drug delivery applications for two reasons. Firstly, targeting can be achieved because the focused ultrasound beam which causes drug release directs energy uniquely at the tumor so only UCA passing through the beam discharge payload and secondly because of the beneficial bio-physical effects including primary radiation forces that drive UCAs toward the vessel wall (28), enhanced vascular permeability and improved cellular drug uptake (1,3). The delivery vehicle discussed here consists of a Dox loaded polymeric UCA. Ultrasound triggered destruction of PLA agents can results in drug-loaded polymer fragments of less than 400 nm diameter, capable of escaping the leaky tumor vasculature and accumulating within the interstitium (15). The polymer is biodegradable and the fragments are capable of releasing incorporated drug over time.

This study shows that encapsulation of Dox in UCAs results in significant reduction of plasma concentrations compared to free Dox (Figure 2). Reducing plasma concentrations of Dox has been shown to be essential for reducing cardiotoxicity and improving the therapeutic index (17). Drug loaded UCAs are also able to significantly reduce the amount of Dox accumulated within the myocardium compared to free Dox confirming the benefits of encapsulation while NP appeared to aggregate within the myocardium resulting in greater drug levels in the myocardium than free Dox (Figure 3E).

Drug levels within the lungs were not significantly different among any of the groups (Figure 3D), indicating that drug loaded UCA is able to pass through the lungs without getting trapped in the pulmonary capillaries, a key requirement for an UCA (29).

Drug levels in the spleen and liver of rats treated with UCAs and NP were significantly greater than those treated with free Dox (Figures 3A, B and C). This accumulation within the spleen and liver is believed to be caused by a rapid uptake of particles by the mononuclear phagocyte system (30). This phenomenon is common among NP and liposomes less than 5 μm with unmodified surfaces (24, 31–32). Opsonins can adsorb to the surface of particles where they interact with macrophage surface receptors and trigger phagocytosis (30). Rahman et al. have reported that mice treated with Dox loaded liposomes have drug levels in the spleen 10 fold greater than those treated with free Dox but with no difference in spleen toxicity compared to free Dox (32). It may be advantageous in the future to modify the surface of the UCAs used in this study with poly(ethylene glycol), poloxamer or vitamin E TPGS, to prevent opsonisation and thus avoid the mononuclear phagocyte system and increase the percentage of drug available for delivery to the tumor (30). This strategy potentially would lead to increased drug carriers in circulation and ultimately higher tumoral delivery due to the EPR effect.

Rats treated with Dox loaded contrast agents showed significantly greater drug levels within the tumor after 4 hours compared to rats treated with free Dox ($p= 0.0472$, Figure 3F) demonstrating this platform's effectiveness as a drug delivery vehicle. While drug levels within the spleen, liver, myocardium and lungs all decreased significantly from day 0 to day 14, drug levels within the tumor showed no significant decrease (Figure 4), presumably a result of the tumor's limited lymphatic drainage. The sustained presence of Dox reinforces

the hypothesis that drug loaded polymer fragments are lodging within the tumor interstitium, presumably a combined consequence of both the EPR effect and biophysical effects of cavitating UCAs. Although not the focus of this study, it was also observed that, 14 days after treatment, tumors treated with UCAs had significantly less growth than tumors treated with free Dox suggesting that the drug is not only in the tumor but also available and active. The concentration of Dox in tumors treated with UCAs was 5.7 μM after 14 days indicating this platform is able to maintain tumoricidal drug concentrations over an extended time frame (33). While the sample size is low (n=3) at 14 days, preliminary results indicate the platform may be effective in halting tumor progression. Others working with drug-loaded embolic beads have compared drug levels at the site with 50% inhibitory concentration (IC50) or a direct cytotoxicity evaluated with the 50% effective concentration (EC50) obtained in cell culture studies (34). Caution must be exercised in comparisons in vitro since Le Bot has shown that human cell lines are 2-fold less sensitive than rat cell lines (35). In vitro studies on five human hepatocellular carcinoma cell lines yielded an average IC_{50} of 0.96 μM (36). In a study in humans with moderately differentiated hepatocellular carcinomas a large variability was noted with the IC_{50} for Dox measured in a range from 4.4 μM to 0.02 μM, and EC_{50} from >17 μM to 0.86 μM (37). We have shown that injection of 12 mg of UCA containing 167 μg Dox resulted in deposition of 4.174 ± 0.840 ng/mg tissue, and these levels did not drop significantly over the 14 day experimental period (day 14 3.478 ± 1.809 ng/mg tissue $p = 0.7$). A complete tabulation of actual Dox levels in ng/mg tissue resulting from insonated UCA is given in table 1.

Autoradiography of tumor sections showed that the majority of Dox was restricted to the periphery of the tumor. The penetration of UCAs into the center of the tumor may have been restricted by high inter-tumoral pressure or by poor vascularization of necrotic regions within the tumor. The agent's penetration into the tumor may also be enhanced by using a more sophisticated ultrasound regimen (28, 38). It may be advantageous to track contrast agents with low intensity ultrasound as they perfuse through the tumor vasculature, then emit a high intensity destructive pulse to destroy the agent throughout the tumor similar to flash replenishment sequences used for perfusion imaging (38). This process may allow intact contrast agent to travel deeper into the tumor before being activated with ultrasound, and thus increase the amount of drug deposited within the tumor.

Conclusion

A Dox loaded UCA capable of being fragmented with external focused ultrasound has been tested in a rat liver cancer model and compared with drug loaded NP and free Dox. UCAs were able to reduce peak plasma drug concentrations, and showed the most efficient delivery of Dox to the tumor compared to other treatment groups. In addition, drug levels in healthy organs dropped from day 0 to day 14 while tumorcidal concentrations of Dox were maintained in the tumor. While the preliminary sample size was limited and this was primarily a study comparing biodistribution of regular and ultrasound-generated NP, we did observe that tumors treated with UCA did not show a significant increase in size over the 14 day study period and were significantly smaller than tumors treated with free Dox which did show an increase in size at 14 days after treatment.

Abbreviations

NP	Nanoparticles
EPR	Enhanced permeability and retention
UCA	Ultrasound contrast agent

Dox	Doxorubicin
PLA	Poly (lactic acid)
%ID	% of injected dose

Acknowledgments

The authors are grateful to Dr. Uwe Haberkorn (German Cancer Research Center in Heidelberg, Germany) for the generous gift of the Morris 3924a hepatoma cell line. We thank Marion Knaus, Karla Carlisle and Lee Shuman for invaluable assistance with animal work. We are indebted to Cameron Koch and Tim Jenkins for the use of and guidance with the Cryostat. Dr. Chaitanya Divigi and Catherine Hou were exceptional for their expert assistance with autoradiography

References

1. Maeda H, Wu J, Sawa T, et al. Tumor vascular permeability and the EPR effect in macromolecular therapeutics: a review. J Control Release. 2000; 65(1–2):271–284. [PubMed: 10699287]
2. Hobbs SK, Monsky WL, Yuan F, et al. Regulation of transport pathways in tumor vessels: role of tumor type and microenvironment. Proc Natl Acad Sci U S A. 1998; 95(8):4607–4612. [PubMed: 9539785]
3. Vaupel P. Tumor microenvironmental physiology and its implications for radiation oncology. Semin Radiat Oncol. 2004; 14(3):198–206. [PubMed: 15254862]
4. Ferrara K, Pollard R, Borden M. Ultrasound microbubble contrast agents: fundamentals and application to gene and drug delivery. Annu Rev Biomed Eng. 2007; 9:415–447. [PubMed: 17651012]
5. Eisenbrey JR, Forsberg F. Contrast-enhanced ultrasound for molecular imaging of angiogenesis. Eur J Nucl Med Mol Imaging. 2010; 37:138–146.
6. Ferrara KW. Driving delivery vehicles with ultrasound. Adv Drug Deliv Rev. 2008; 60(10):1097–1102. [PubMed: 18479775]
7. Bekeredjian R, Katus HA, Kuecherer HF. Therapeutic use of ultrasound targeted microbubble destruction: a review of non-cardiac applications. Ultraschall Med. 2006; 27(2):134–140. [PubMed: 16612722]
8. Price RJ, Skyba DM, Kaul S, et al. Delivery of colloidal particles and red blood cells to tissue through microvessel ruptures created by targeted microbubble destruction with ultrasound. Circulation. 1998; 98(13):1264–1267. [PubMed: 9751673]
9. Tinkov S, Winter G, Coester C, et al. New doxorubicin-loaded phospholipid microbubbles for targeted tumor therapy: Part I--Formulation development and in-vitro characterization. J Control Release. 2010; 143(1):143–150. [PubMed: 20060861]
10. Husseini GA, Diaz de la Rosa MA, Gabuji T, et al. Release of doxorubicin from unstabilized and stabilized micelles under the action of ultrasound. J Nanosci Nanotechnol. 2007; 7(3):1028–1033. [PubMed: 17450870]
11. Gao Z-G, Fain HD, Rapoport N. Controlled and targeted tumor chemotherapy by micellar-encapsulated drug and ultrasound. J Control Release. 2005; 102(1):203–222. [PubMed: 15653146]
12. Kheirolomoom A, Dayton PA, Lum AFH, et al. Acoustically-active microbubbles conjugated to liposomes: characterization of a proposed drug delivery vehicle. J Control Release. 2007; 118(3):275–284. [PubMed: 17300849]
13. Jones M, Leroux J. Polymeric micelles - a new generation of colloidal drug carriers. Eur J Pharm Biopharm. 1999; 48(2):101–111. [PubMed: 10469928]
14. Alberts DS, Garcia DJ. Safety aspects of pegylated liposomal doxorubicin in patients with cancer. Drugs. 1997; 54 Suppl 4:30–35. [PubMed: 9361959]
15. Kooiman K, Bohmer MR, Emmer M, et al. Oil-filled polymer microcapsules for ultrasound-mediated delivery of lipophilic drugs. J Control Release. 2009; 133(2):109–118. [PubMed: 18951931]

16. Eisenbrey JR, Burstein OM, Kambhampati R, et al. Development and optimization of a doxorubicin loaded poly(lactic acid) contrast agent for ultrasound directed drug delivery. J Control Release. 2010; 143(1):38–44. [PubMed: 20060024]
17. El-Sherif DM, Wheatley MA. Development of a novel method for synthesis of a polymeric ultrasound contrast agent. J Biomed Mater Res A. 2003; 66(2):347–355. [PubMed: 12889005]
18. Eisenbrey JR, Huang P, Hsu J, et al. Ultrasound triggered cell death in vitro with doxorubicin loaded poly lactic-acid contrast agents. Ultrasonics. 2009; 49(8):628–633. [PubMed: 19394992]
19. Eisenbrey JR, Soulen MC, Wheatley MA. Delivery of encapsulated Doxorubicin by ultrasound-mediated size reduction of drug-loaded polymer contrast agents. IEEE Trans Biomed Eng. 2010; 57(1):24–28. [PubMed: 19709952]
20. Gewirtz DA. A critical evaluation of the mechanisms of action proposed for the antitumor effects of the anthracycline antibiotics adriamycin and daunorubicin. Biochem Pharmacol. 1999; 57(7): 727–741. [PubMed: 10075079]
21. Singal PK, Iliskovic N. Doxorubicin-induced cardiomyopathy. N Engl J Med. 1998; 339(13):900–905. [PubMed: 9744975]
22. Gabizon A, Catane R, Uziely B, et al. Prolonged circulation time and enhanced accumulation in malignant exudates of doxorubicin encapsulated in polyethylene-glycol coated liposomes. Cancer Res. 1994; 54(4):987–992. [PubMed: 8313389]
23. Nishiyama N, Kataoka K. Current state, achievements, and future prospects of polymeric micelles as nanocarriers for drug and gene delivery. Pharmacol Ther. 2006; 112(3):630–648. [PubMed: 16815554]
24. Brigger I, Dubernet C, Couvreur P. Nanoparticles in cancer therapy and diagnosis. Adv Drug Deliv Rev. 2002; 54(5):631–651. [PubMed: 12204596]
25. Tewes F, Munnier E, Antoon B, et al. Comparative study of doxorubicin-loaded poly(lactide-co-glycolide) nanoparticles prepared by single and double emulsion methods. Eur J Pharm Biopharm. 2007; 66(3):488–492. [PubMed: 17433641]
26. Maataoui A, Qian J, Vossoughi D, et al. Transarterial chemoembolization alone and in combination with other therapies: a comparative study in an animal HCC model. Eur Radiol. 2005; 15(1):127–133. [PubMed: 15580507]
27. Yang R, Rescorla FJ, Reilly CR, et al. A reproducible rat liver cancer model for experimental therapy: introducing a technique of intrahepatic tumor implantation. J Surg Res. 1992; 52(3):193–198. [PubMed: 1538593]
28. Lum AF, Borden MA, Dayton PA, et al. Ultrasound radiation force enables targeted deposition of model drug carriers loaded on microbubbles. J Control Release. 2006; 111(1–2):128–134. [PubMed: 16380187]
29. Goldberg BB, Liu JB, Forsberg F. Ultrasound contrast agents: a review. Ultrasound Med Biol. 1994; 20(4):319–333. [PubMed: 8085289]
30. Storm G, Belliot SO, Daemen T, et al. Surface modification of nanoparticles to oppose uptake by the mononuclear phagocyte system. Adv Drug Deliv Rev. 1995; (17):31–48.
31. Brannon-Peppas L, Blanchette JO. Nanoparticle and targeted systems for cancer therapy. Adv Drug Deliv Rev. 2004; 56(11):1649–1659. [PubMed: 15350294]
32. Rahman A, Ganjei A, Neefe JR. Comparative immunotoxicity of free doxorubicin and doxorubicin encapsulated in cardiolipin liposomes. Cancer Chemother Pharmacol. 1986; 16(1):28–34. [PubMed: 3484382]
33. Minotti G, Menna P, Salvatorelli E, et al. Anthracyclines: molecular advances and pharmacologic developments in antitumor activity and cardiotoxicity. Pharmacol Rev. 2004; 56(2):185–229. [PubMed: 15169927]
34. Namur J, Wassef M, Millot J-M, et al. Drug-eluting Beads for Liver Embolization: Concentration of Doxorubicin in Tissue and in Beads in a Pig model. J Vasc Interv Radiol. 2010; 21:259–267. [PubMed: 20123210]
35. Le Bot MA, Begue JM, Kernaleguen D, et al. Different cytotoxicity and metabolism of doxorubicin, daunorubicin, epirubicin, esorubicin and idarubicin in cultured human and rat hepatocytes. Biochem Pharmacol. 1988; 37:3877–3887. [PubMed: 3190734]

36. Yuan S, Zhang X, Lu L, et al. Anticancer activity of methoxymorpholinyl doxorubicin (PNU 152243) on human hepatocellular carcinoma. Anticancer Drugs. 2004; 15:641–646. [PubMed: 15205610]

37. Chuu JJ, Liu JM, Tsou MH, et al. Effects of paclitaxel and doxorubicin in histocultures of hepatocellular carcinomas. J Biomed Sci. 2007; 14:233–244. [PubMed: 17206490]

38. Schlosser T, Pohl C, Veltmann C, et al. Feasibility of the flash-replenishment concept in renal tissue: which parameters affect the assessment of the contrast replenishment? Ultrasound Med Biol. 2001; 27(7):937–944. [PubMed: 11476928]

39. Shortencarier MJ, Dayton PA, Bloch SH, et al. A Method for Radiation-Force Localized Drug Delivery Using Gas-Filled Lipospheres. IEEE Trans Ultrasonics, Ferroelectrics, Frequency Control. 2004; 51(7):222–831.

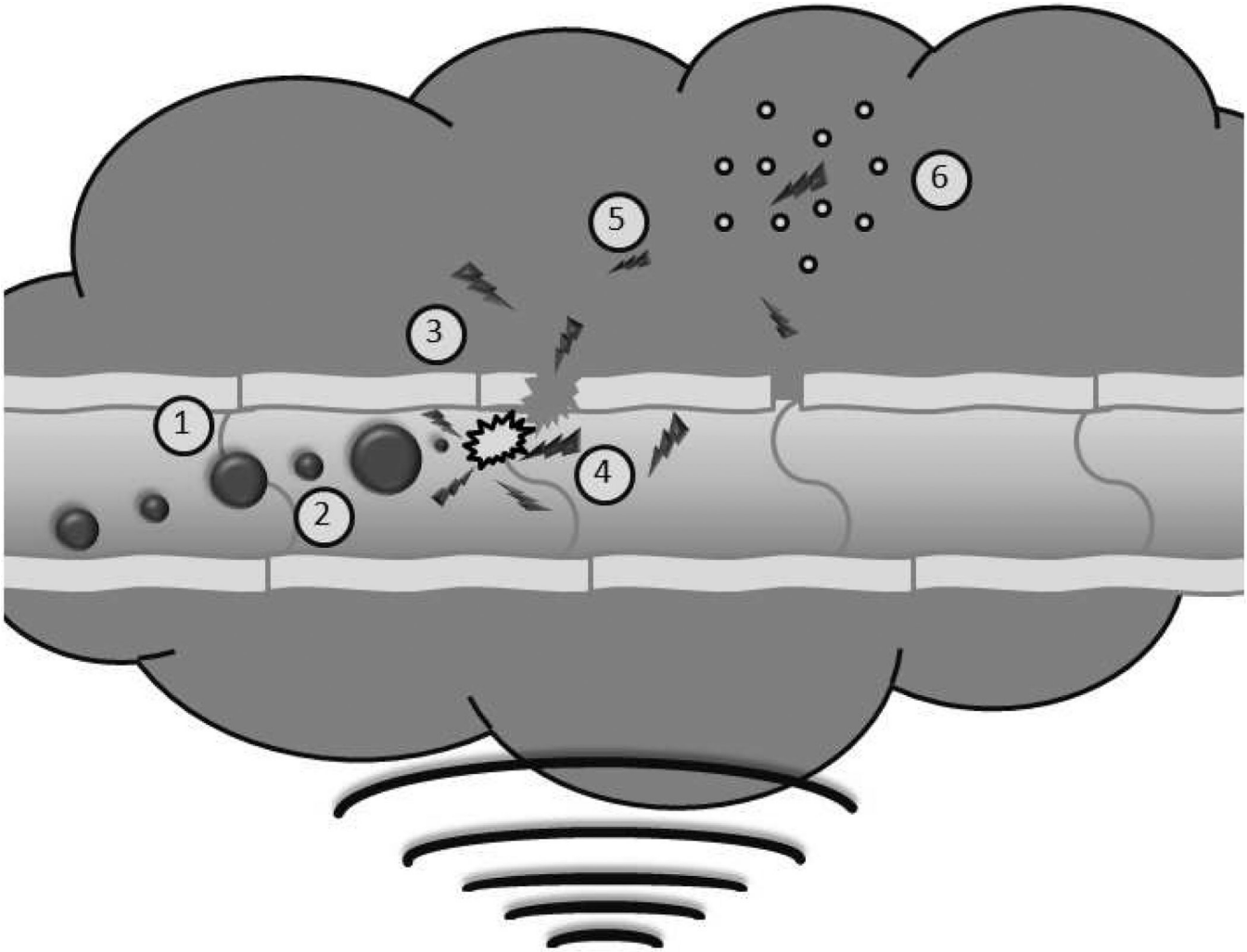

Figure 1.

Schematic of ultrasound triggered drug delivery. Doxorubicin loaded UCAs pass freely through the vasculature until exposed to ultrasound where they experience (1) acoustic radiation forces that push the microbubbles to the vessel wall. The oscillating pressure wave will also lead to (2) microbubble cavitation as the gas core expands and contracts in response to changes in pressure. When exposed to sufficiently strong ultrasound pulses, the microbubble will undergo (3) inertial cavitation resulting in the destruction of the polymer shell, creating drug loaded polymer fragments less than 400 nm. The energy released in the process of microbubble destruction is sufficient to (4) enhance the permeability of the vessel wall. The fragments can then begin to (5) accumulate within the tumor interstitium, potentially, through acoustic radiation force [39] and with time, circulating fragments will accumulate though the enhanced permeability and retention effect. Lodged polymer fragments can (6) slowly degrade providing a sustained localized release of the chemotherapeutic agent.

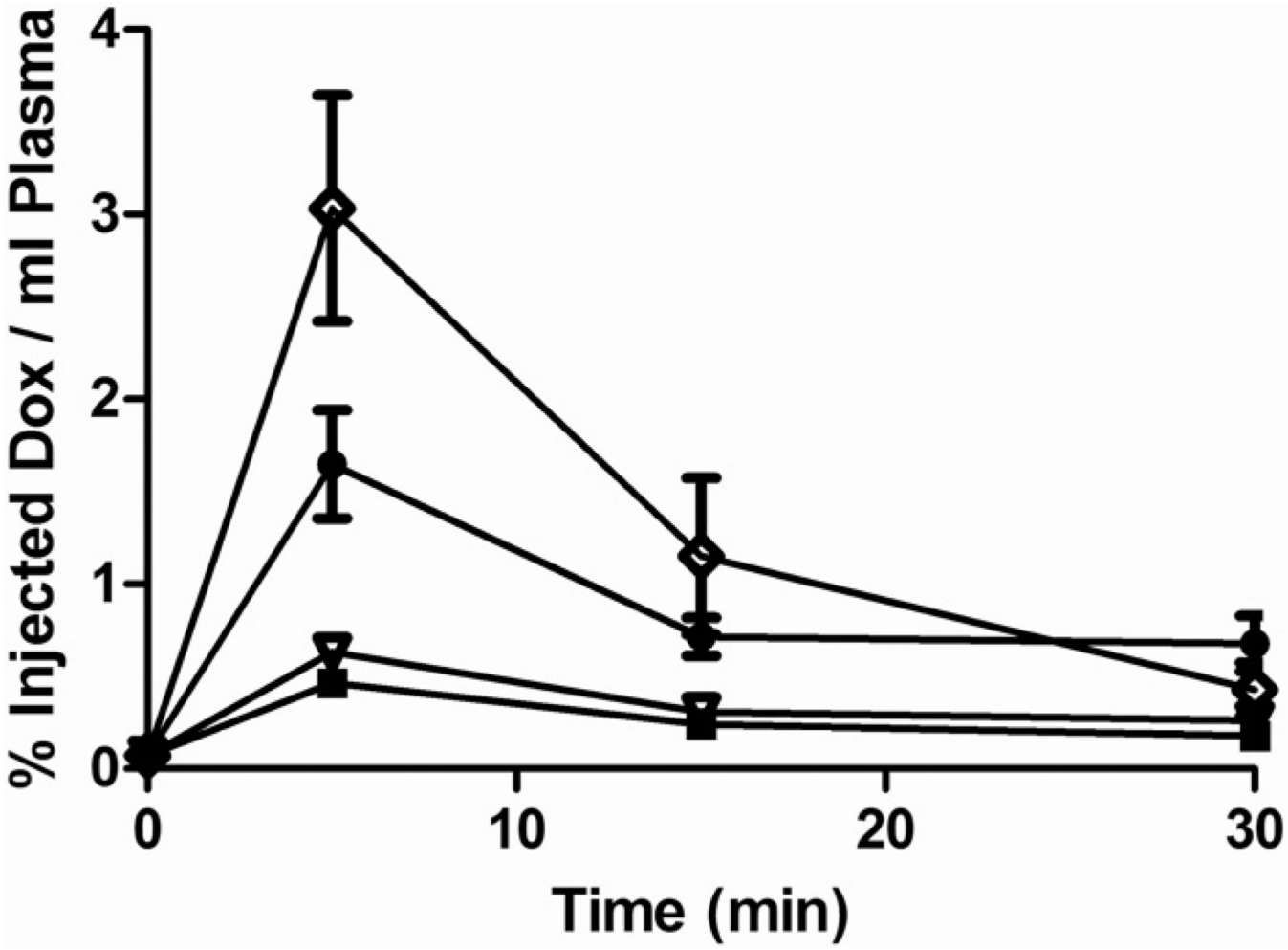

Figure 2.

Effect of delivery vehicle on the concentration of doxorubicin in plasma. Vehicles include: 12 mg UCA, 12 mg nanoparticles, a combination of 6 mg nanoparticles and 6 mg UCA or free doxorubicin. After 5 minutes plasma drug concentrations were significantly greater in rats treated with free doxorubicin compared to all other treatments ($p<0.0470$) and concentrations were significantly greater in rats treated with nanoparticles compared to UCAs ($p=0.0052$). n=5

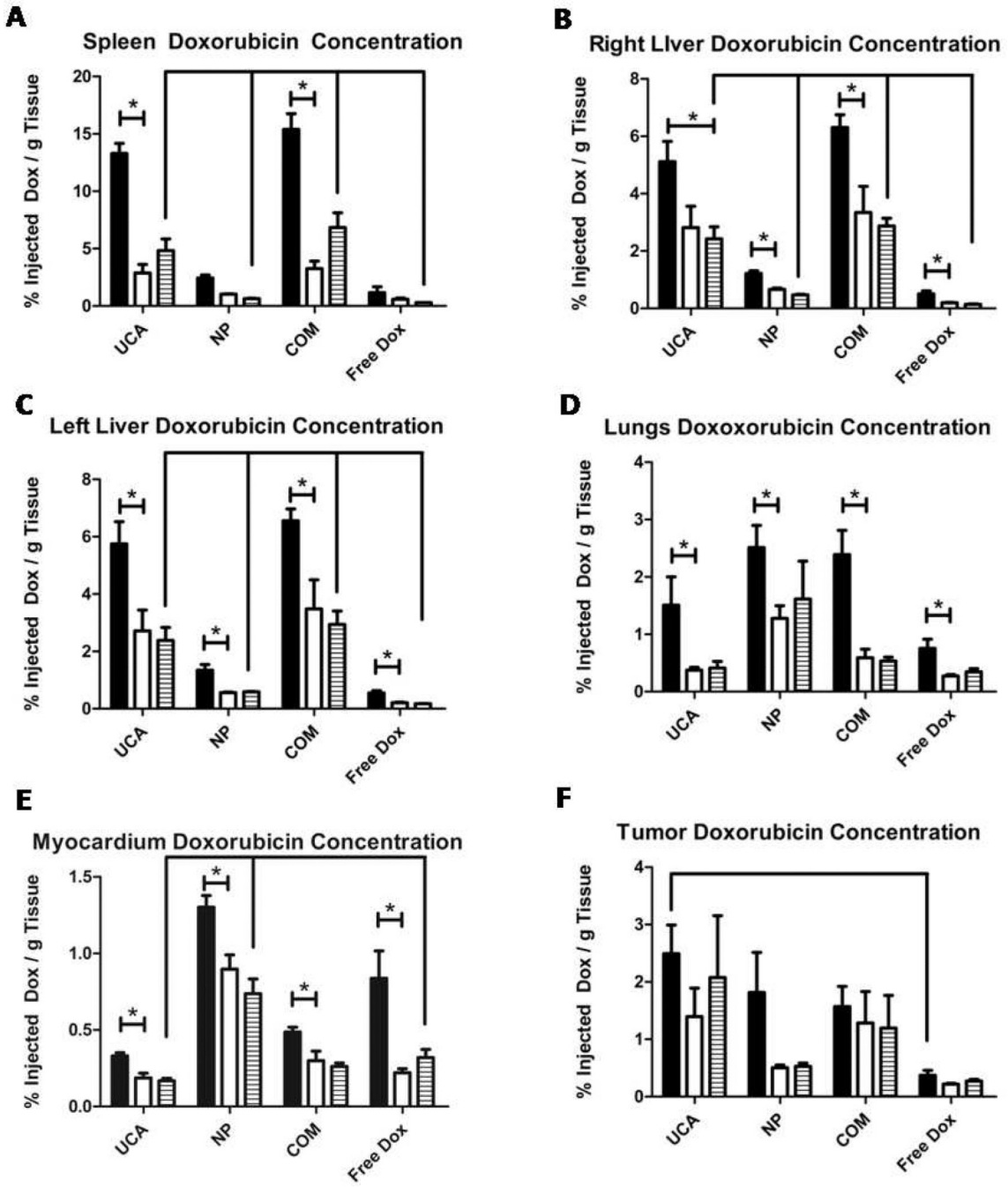

Figure 3.

The effect of vehicle type on the distribution of doxorubicin in animals. Vehicle is comprised of: UCA (12 mg), nanoparticles (NP) (12 mg), a combination of 6 mg UCA and 6 mg nanoparticles (COM), and free doxorubicin (Free Dox) (112 μg). A) spleen B) right lobe of the liver C) left lobe of the liver D) lungs E) myocardium and F) tumor. Samples were quantified at 4 hours ■, 7 days ⊏ and 14 days ⊆ after treatment. Doxorubicin levels for all four treatment groups dropped after the 4 hour time point in all healthy organs but not in the tumor (*$p<0.0368$).

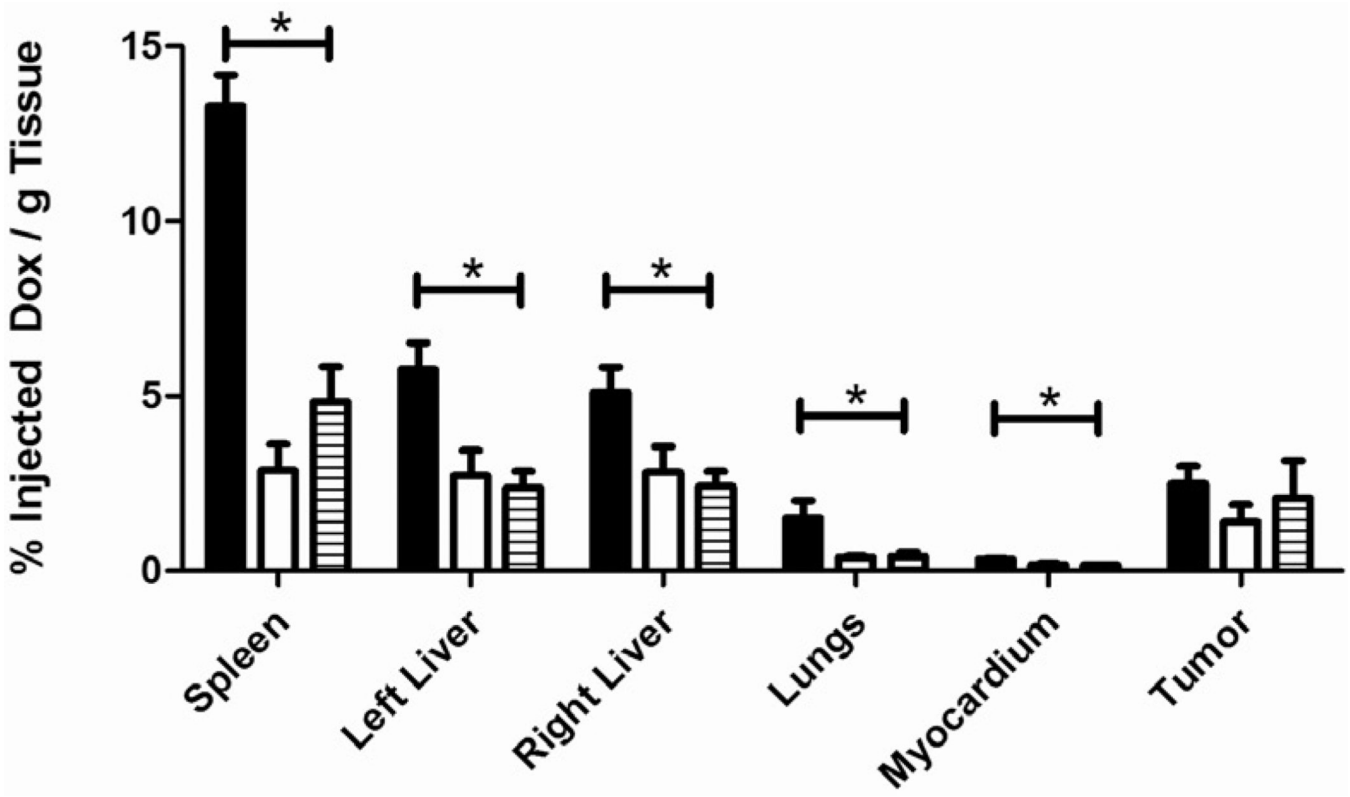

Figure 4.

The biodistribution of doxorubicin loaded UCAs. Samples were quantified at 4 hours ■, 7 days ⊏ and 14 days ⊑ after treatment. Drug levels in the spleen, liver, lungs and myocardium all peaked at 4 hours and dropped significantly after 14 days ($p<0.0212$) while drug levels in the tumor showed no significant drop in drug levels from day 0 to day 14 ($p=0.7$).

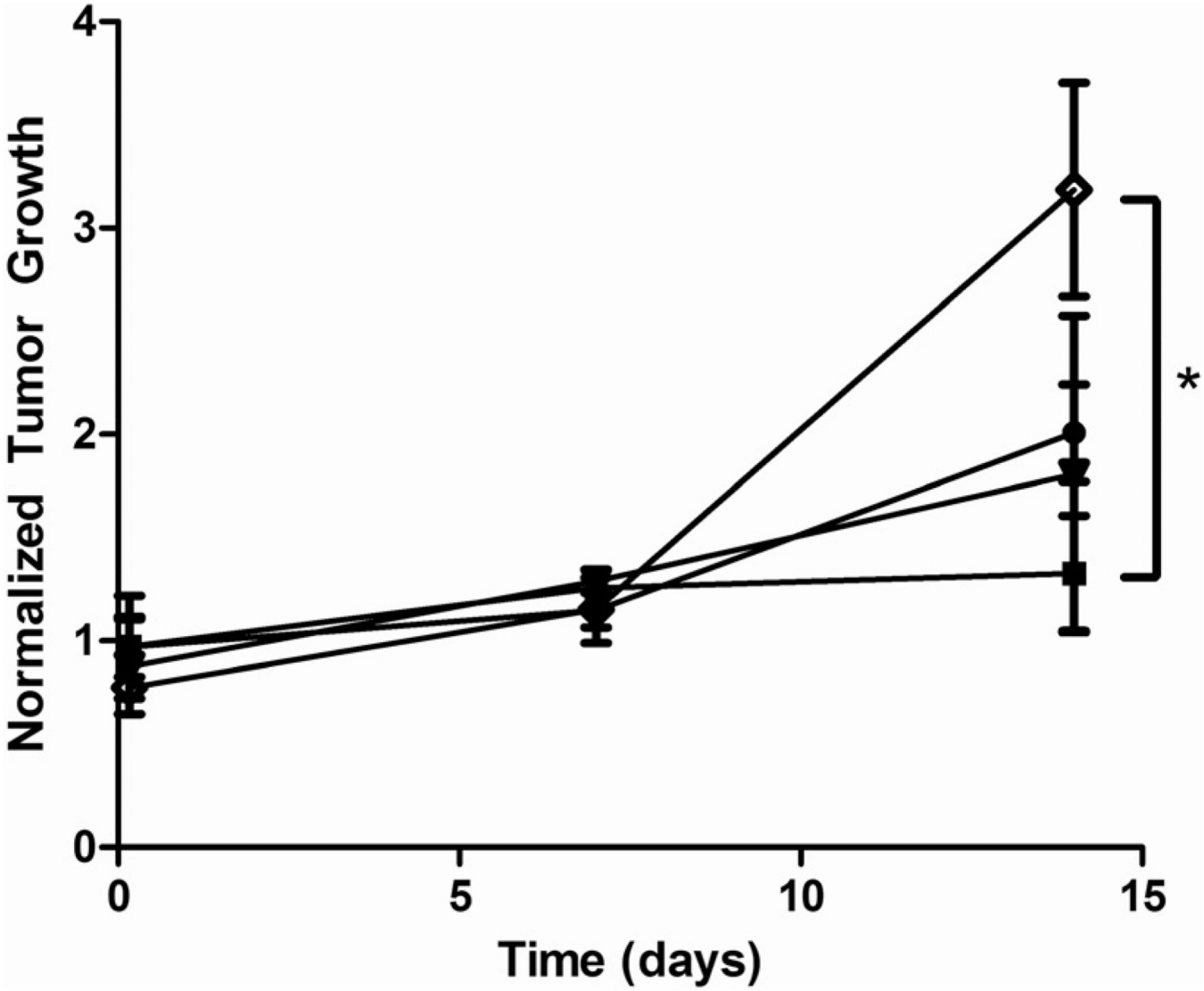

Figure 5.

Effect of vehicle on tumor growth in rats. Vehicles include; 12 mg UCA, 12 mg nanoparticles, a combination of 6 mg nanoparticles and 6 mg UCA or free doxorubicin. All rats were insonated for 20 minutes after injection. Tumors treated with UCA did not show a significant increase in size over 14 days (p=0.3) and had significantly less growth than rats treated with free doxorubicin after 14 days (p=0.0390).

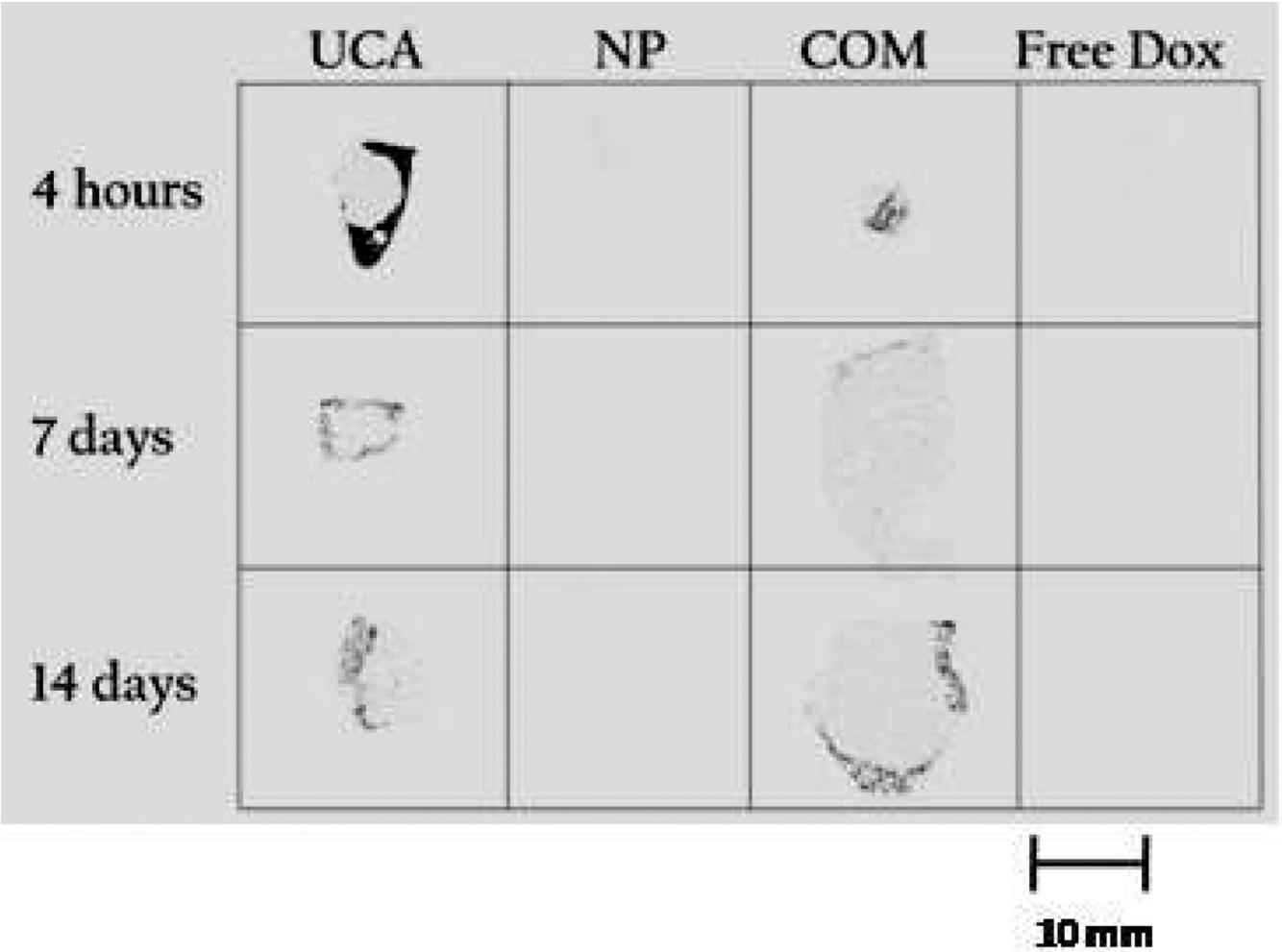

Figure 6.
Effect of vehicle on drug distribution in the tumor with time. Autoradiography images of tumors treated with 12 mg ultrasound contrast agent, 12 mg nanoparticles (NP), a combination of 6 mg nanoparticles and 6 mg UCA (COM) or free doxorubicin (Free Dox) and sacrificed after 4 hours, 7 days or 14 days. Size bar = 10 mm

Table 1

ActualDrug levels generated by ultrasound treatment of drug loaded contrast agent

Time	Myocardium (ng/mg tissue)	Spleen (ng/mg tissue)	Left Liver (ng/mg tissue)	Right Liver (ng/mg tissue)	Lungs (ng/mg tissue)	Tumor (ng/mg tissue)
4 hours	0.554 ± 0.035	22.272 ± 1.482	9.637 ± 1.297	8.577 ± 1.179	2.525 ± 0.832	4.174 ± 0.840
7 days	0.314 ± 0.052	4.815 ± 1.250	4.552 ± 1.213	4.718 ± 1.248	0.630 ± 0.081	2.340 ± 0.829
14 days	0.281 ± 0.028	8.099 ± 1.679	3.99 ± 0.767	4.061 ± 0.699	0.688 ± 0.199	3.478 ± 1.809